

can be separated biochemically, and the former can be further subdivided into base, which contains Rpt1-6, Rpn1, and Rpn2 and exhibits chaperonin activity (21, 22), and lid (16, 17). However, there has been no previous evidence that these subspecies represent physiologically relevant complexes. Our results suggest that there is at least one discrete subcomplex of the 19S and that it functions independently of other proteasome subunits in Gal4-mediated transcription. This species, which we call the APIS (AAA proteins independent of 20S) complex, clearly includes the six 19S ATPases (Rpt1 to Rpt6) and perhaps other proteins. The precise composition of the APIS complex, and whether it corresponds to the biochemically defined base, remains to be elucidated.

There has been increasing evidence of a link between ubiquitylation and transcription (23–26). Recent work by Tansey and colleagues suggests a mechanism by which they might be linked temporally. They found that for the artificial LexA-VP16 activator, ubiquitylation of the activator is required for the activator to function in yeast (26). Importantly, linkage of a single ubiquitin molecule to the activator was shown to lead to activation, but did not signal proteolytic turnover. This suggests that it is ubiquitylation per se, and not ubiquitin-linked proteolysis, that is crucial for activator function. Whereas the Gal4 AD alone is capable of binding the APIS complex (Fig. 3), an attached monoubiquitin might enhance this interaction or modulate the activity of the AD-bound complex in a way that is important for transcription to proceed. After induction, the ubiquitin chain on the activator would grow, possibly signaling a switch in activator association from the APIS complex to the full 26S proteasome. The time required for the ubiquitin chain to reach the minimum size needed to signal proteasome-mediated degradation (27) would be used by Gal4 to drive high-level transcription. But after that time, the activator would be subject to degradation, thus placing a “governor” on gene expression. The critical element of this model is that mono- and polyubiquitin chains are fundamentally different modifications that signal different intermolecular interactions. Although speculative, we believe that this model is useful in potentially linking a number of notable recent findings and in providing a number of readily testable hypotheses.

References and Notes

1. W. Baumeister, J. Walz, F. Zuhl, E. Seemuller, *Cell* **92**, 367 (1998).
2. M. H. Glickman, D. M. Rubin, V. A. Fried, D. Finley, *Mol. Cell. Biol.* **18**, 3149 (1998).
3. F. Confalonieri, M. Duguet, *BioEssays* **17**, 639 (1995).
4. J. C. Swaffield, J. Bromberg, S. A. Johnston, *Nature* **357**, 698 (1992).
5. K. Melcher, S. Johnston, *Mol. Cell. Biol.* **15**, 2839 (1995).
6. C. Chang et al., *J. Biol. Chem.* **276**, 30956 (2001).
7. A. Ferdous, F. Gonzalez, L. Sun, T. Kodadek, S. A. Johnston, *Mol. Cell* **7**, 981 (2001).
8. D. Rubin et al., *Nature* **379**, 655 (1996).

9. K. Ferrell, C. R. M. Wilkinson, W. Dubiel, C. Gordon, *Trends Biochem. Sci.* **25**, 83 (2000).
10. G. Orphanides, W.-H. Wu, W. S. Lane, M. Hampsey, D. Reinberg, *Nature* **400**, 284 (1999).
11. P. C. Dedon, J. A. Soultz, C. D. Allis, M. A. Gorovsky, *Anal. Biochem.* **197**, 83 (1991).
12. S. A. Johnston, J. E. Hopper, *Proc. Natl. Acad. Sci. U.S.A.* **79**, 6971 (1982).
13. D. Lohr, P. Venkov, J. Zlatanova, *FASEB J.* **9**, 777 (1995).
14. F. Gonzalez, A. Delahodde, T. Kodadek, S. Albert Johnston, data not shown.
15. Supplementary figures and details of experimental procedures are available on Science Online at www.sciencemag.org/cgi/content/full/296/5567/548/DC1.
16. M. H. Glickman et al., *Cell* **94**, 615 (1998).
17. Y. Saeki, A. Toh-e, H. Yokosawa, *Biochem. Biophys. Res. Commun.* **273**, 509 (2000).
18. C. Schaubert et al., *Nature* **391**, 715 (1998).
19. The RPT genes were amplified by PCR from yeast genomic DNA and cloned into the in vitro transcription vector pTL37N. The resultant RNA was then translated with the TNT rabbit reticulocyte system (Promega).

20. J. C. Carrington, T. D. Parks, S. M. Cary, W. G. Dougherty, *Nucleic Acids Res.* **15**, 10066 (1987).
21. B. C. Braun et al., *Nature Cell Biol.* **1**, 221 (1999).
22. E. Strickland, K. Hakala, P. J. Thomas, G. N. DeMartino, *J. Biol. Chem.* **275**, 5565 (2000).
23. E. Molinari, M. Gilman, S. Natesan, *EMBO J.* **18**, 6439 (1999).
24. S. E. Salghetti, S. Y. Kim, W. P. Tansey, *EMBO J.* **18**, 717 (1999).
25. S. E. Salghetti, M. Muratani, H. Wijnen, B. Futcher, W. P. Tansey, *Proc. Natl. Acad. Sci. U.S.A.* **97**, 3118 (2000).
26. S. E. Salghetti, A. A. Caudy, J. G. Chenoweth, W. P. Tansey, *Science* **293**, 1651 (2001).
27. J. S. Thrower, L. Hoffman, M. Rechsteiner, C. M. Pickart, *EMBO J.* **19**, 94 (2000).
28. We thank J. Swaffield (North Carolina State University) for antibodies raised against Rpt1-3 and Rpt-5, and A. Toh-e (University of Tokyo) for antibodies raised against Rpn9 and Rpn12. We also thank E. Webb, L. Zhang, and X. Chen for technical assistance. F.G. was supported in part by an NIH training grant. A.D. was supported in part by the CNRS. This work was supported by unrestricted funds of T.K. and S.A.J.

2 January 2002; accepted 6 February 2002

A System for Stable Expression of Short Interfering RNAs in Mammalian Cells

Tijn R. Brummelkamp,¹ René Bernards,^{1,3} Reuven Agami^{1,2,3*}

Mammalian genetic approaches to study gene function have been hampered by the lack of tools to generate stable loss-of-function phenotypes efficiently. We report here a new vector system, named pSUPER, which directs the synthesis of small interfering RNAs (siRNAs) in mammalian cells. We show that siRNA expression mediated by this vector causes efficient and specific down-regulation of gene expression, resulting in functional inactivation of the targeted genes. Stable expression of siRNAs using this vector mediates persistent suppression of gene expression, allowing the analysis of loss-of-function phenotypes that develop over longer periods of time. Therefore, the pSUPER vector constitutes a new and powerful system to analyze gene function in a variety of mammalian cell types.

In several organisms, introduction of double-stranded RNA has proven to be a powerful tool to suppress gene expression through a process known as RNA interference (1). However, in most mammalian cells this provokes a strong cytotoxic response (2). This non-specific effect can be circumvented by use of synthetic short [21- to 22-nucleotide(nt) interfering RNAs (siRNAs)], which can mediate strong and specific suppression of gene expression (3). However, this reduction in gene expression is transient, which severely restricts its applications. To overcome this limitation, we designed a mammalian expression vector that directs the synthesis of siRNA-like transcripts [pSUPER,

suppression of endogenous RNA, Fig. 1A and Supplementary fig. 1C (4)]. We used the polymerase-III H1-RNA gene promoter, as it produces a small RNA transcript lacking a polyadenosine tail and has a well-defined start of transcription and a termination signal consisting of five thymidines in a row (T5). Most important, the cleavage of the transcript at the termination site is after the second uridine (5) yielding a transcript resembling the ends of synthetic siRNAs, which also contain two 3' overhanging T or U nucleotides (nt) (Fig. 1A). We designed the gene-specific insert such that it specifies a 19-nt sequence derived from the target transcript, separated by a short spacer from the reverse complement of the same 19-nt sequence. The resulting transcript is predicted to fold back on itself to form a 19-base pair stem-loop structure, resembling that of *C. elegans Let-7* (Fig. 1A).

We used the pSUPER vector to suppress the endogenous *CDH1* gene, an activator of

¹Division of Molecular Carcinogenesis, ²Division of Tumor Biology, The Netherlands Cancer Institute, Plesmanlaan 121, 1066 CX Amsterdam, Netherlands. ³Center for Biomedical Genetics, Netherlands.

*To whom correspondence should be addressed. E-mail: r.agami@nki.nl

REPORTS

the anaphase-promoting complex (APC). We designed three related vectors directing the synthesis of the same 19-base pair double-stranded *CDH1* target sequence, containing loops of seven, nine, or five nucleotides (Fig. 1A, constructs A, B, and C, respectively). We compared the ability of these vectors to inhibit *CDH1* to that of synthetic siRNA oligonucleotides targeted against the same sequence of *CDH1* (Fig. 1A) in a transient expression experiment in MCF-7 cells. Introduction of *CDH1* synthetic siRNA resulted in a reproducible reduction of more than 90% of CDH1 protein (Fig. 1B, lane 2). Importantly, pSUPER-CDH1-B was able to knockdown *CDH1* expression to the same extent as was seen with the synthetic *CDH1* siRNA (Fig. 1B, lane 5). pSUPER-CDH1-A only had a moderate activity, whereas pSUPER-CDH1-C was inactive in this assay, indicating that the size and nucleotide sequence of the loop is very important. Neither the transfection of the synthetic *CDH1* siRNA, nor introduction of the siRNA expression vector,

had any detrimental effect on cell survival or cell-cycle profile (6).

Next, we examined whether pSUPER vectors produce siRNA. Northern blot analysis revealed that cells transfected with pSUPER-CDH1-B produce both sense and antisense 21- to 22-nt *CDH1* RNAs, which are similar in size to those seen in cells transfected with the synthetic siRNA (Fig. 1C). The 49-nt precursor transcript can be barely detected with both probes, suggesting rapid cleavage to siRNA. (Owing to its strong secondary structure, the precursor transcript migrates around 40-nt.) These results indicate that the stem-loop precursor transcript was generated and cleaved in the cell to produce a functional siRNA.

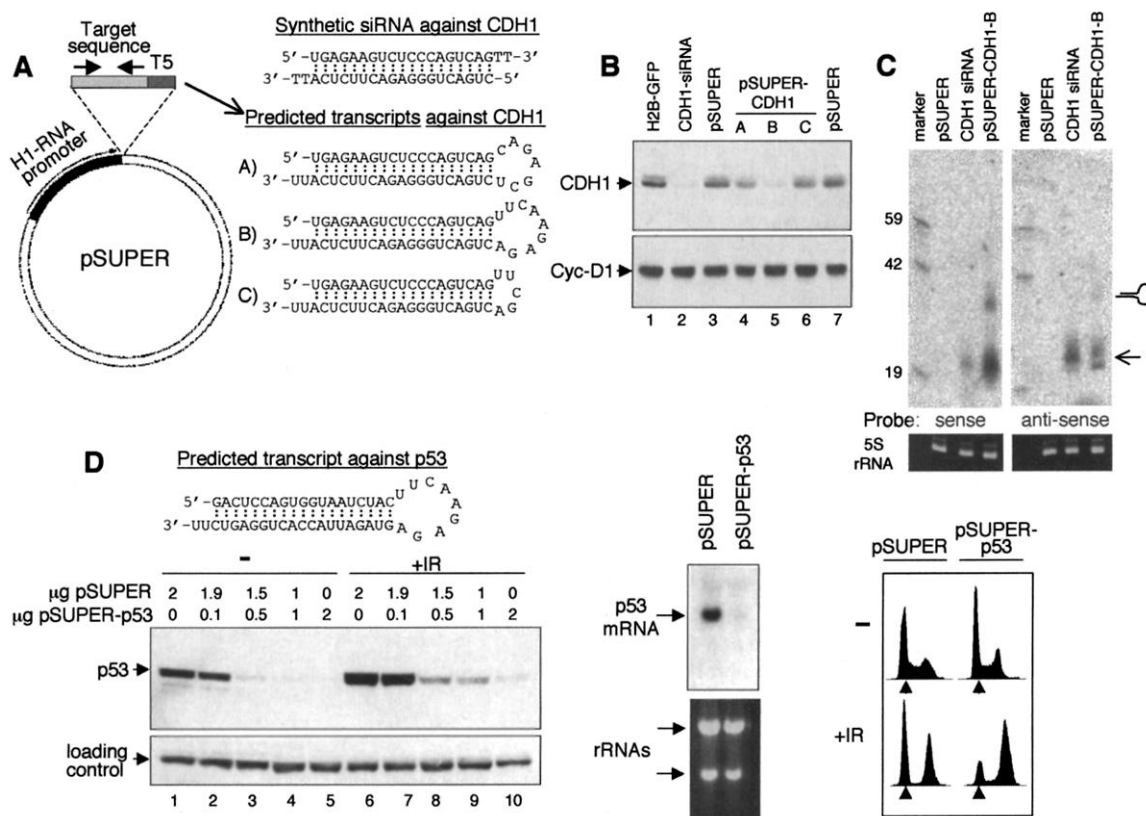
To examine the specificity of our pSUPER system, we constructed two *CDH1* vectors harboring a mutation at either position 2 or 9 of the *CDH1* target recognition sequence (Fig. 2A). Transient transfection of these constructs into cells failed to suppress *CDH1* expression, although both vectors yielded

transcripts of the length of siRNAs [Fig. 2A and (6)]. These results demonstrate that suppression of gene expression by pSUPER system is highly target sequence-specific.

To further test the vector system, we designed both a synthetic siRNA and a pSUPER vector that target the same 19-nt sequence in the *CDC20* transcript. As for *CDH1*, efficient suppression of endogenous *CDC20* expression was achieved with both synthetic siRNA and with pSUPER-*CDC20* (Fig. 2B). To measure the level of gene suppression accurately by the pSUPER system, we designed a construct to target polo like kinase-1 (PLK1). Introduction of pSUPER-PLK1 led to a significant decrease in PLK1 protein levels and a reduction in PLK1 kinase activity by a factor of 10 [Supplementary fig. 1A (4)]. To date, we were successful in knocking down the expression of more than 10 genes for which we designed a pSUPER siRNA vector, highlighting the efficiency with which genes can be targeted using this vector (6).

Next, we asked whether suppression of gene

Fig. 1. A vector-based suppression of gene expression in mammalian cells. (A) Schematic drawing of the pSUPER vector. The H1-RNA promoter was cloned in front of the gene specific targeting sequence (19-nt sequences from the target transcript separated by a short spacer from the reverse complement of the same sequence) and five thymidines (T5) as termination signal. The predicted secondary structures of pSUPER-CDH1 transcripts and the synthetic siRNA used to target *CDH1* are depicted. (B) MCF-7 cells were transfected using an electroporation protocol, which results in more than 90% transfection efficiency (7). The indicated DNA constructs (1 µg) and synthetic siRNA (1.5 µg) were transfected. Sixty



hours later whole-cell extracts were prepared, separated on 10% SDS-polyacrylamide gel electrophoresis (SDS-PAGE) and immunoblotted to detect CDH1 protein. An immunoblot with antibody against cyclin D1 was used as a control. (C) Cells were transfected as described above, and total RNA was extracted 60 hours later. RNA (30 µg) was loaded on a 11% denaturing polyacrylamide gel, separated, and blotted as described (8). Membranes were probed with either ³²P-labeled sense or antisense 19-nt *Cdh1* target oligonucleotide and visualized by PhosphorImager (overnight exposure). The stem-loop precursor and the siRNAs are indicated. The control 5S-rRNA band was detected with ethidium bromide staining. (D) Left, Cells were transfected with

increasing amounts pSUPER-p53, which is predicted to produce the depicted transcript. Sixty hours after transfection cells were either irradiated (+IR, 20 Gy) or left untreated, harvested 2 hours later, and separated on 10% SDS-PAGE. Immunoblot with p53-specific antibody was performed and the bands corresponding to p53 protein and a loading control are indicated. Middle, Northern blot showing levels of p53 mRNA in cells transfected with 1 µg of pSUPER constructs as indicated. Ethidium bromide staining of rRNAs is used as loading control. Right, Flow cytometry was performed on cells transfected with 1 µg plasmids 24 hours after irradiation as described (7). Cells with DNA in the G₁ phase are indicated with an arrow.

REPORTS

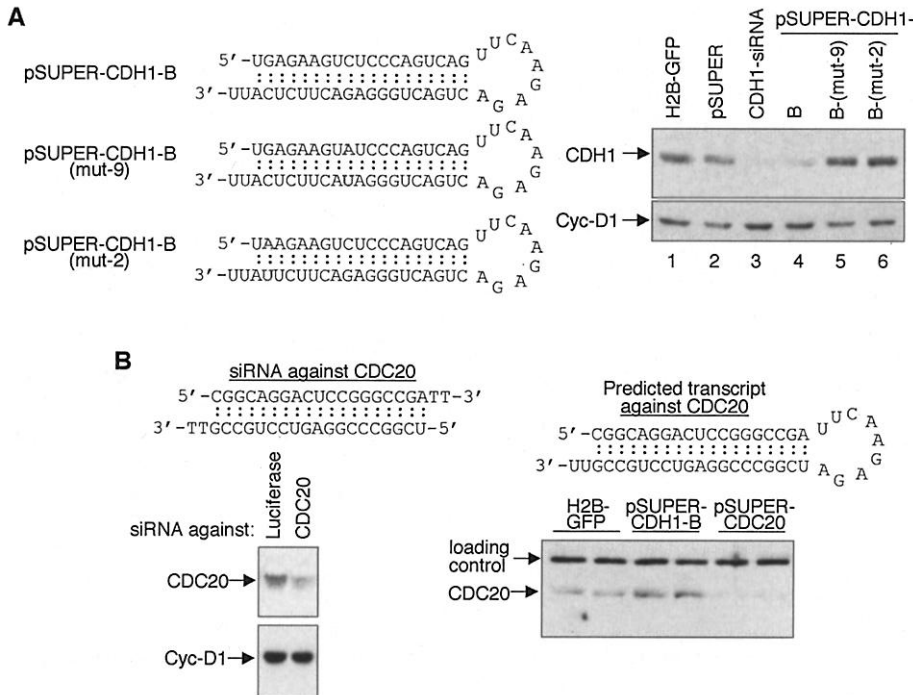


Fig. 2. (A) An intact target recognition sequence is required to suppress CDH1 by pSUPER-CDH1 vector. The *CDH1* 19-nt target-recognition sequence was mutated to give a 1-base pair substitution at either position 9 or 2 of the stem. The predicted secondary structures of the transcripts are shown. U2OS cells were transfected exactly as described in Fig. 1. Whole-cell extracts were prepared after 60 hours, separated on 10% SDS-PAGE, and analyzed by immunoblotting with CDH1-specific antibody. Cyclin D1 protein was used to demonstrate equal loading. **(B)** Suppression of *CDC20* expression by both synthetic siRNA and pSUPER-CDC20. Shown are the sequences of the siRNA and the predicted transcript of pSUPER-CDC20 utilized to knockdown *CDC20* expression. The indicated siRNAs and plasmids were transfected into MCF-7 cells as described above. Whole-cell extracts were separated on 10% SDS-PAGE and immunoblotted to detect CDC20 and cyclin D1 proteins. Two transfections from each vector are shown.

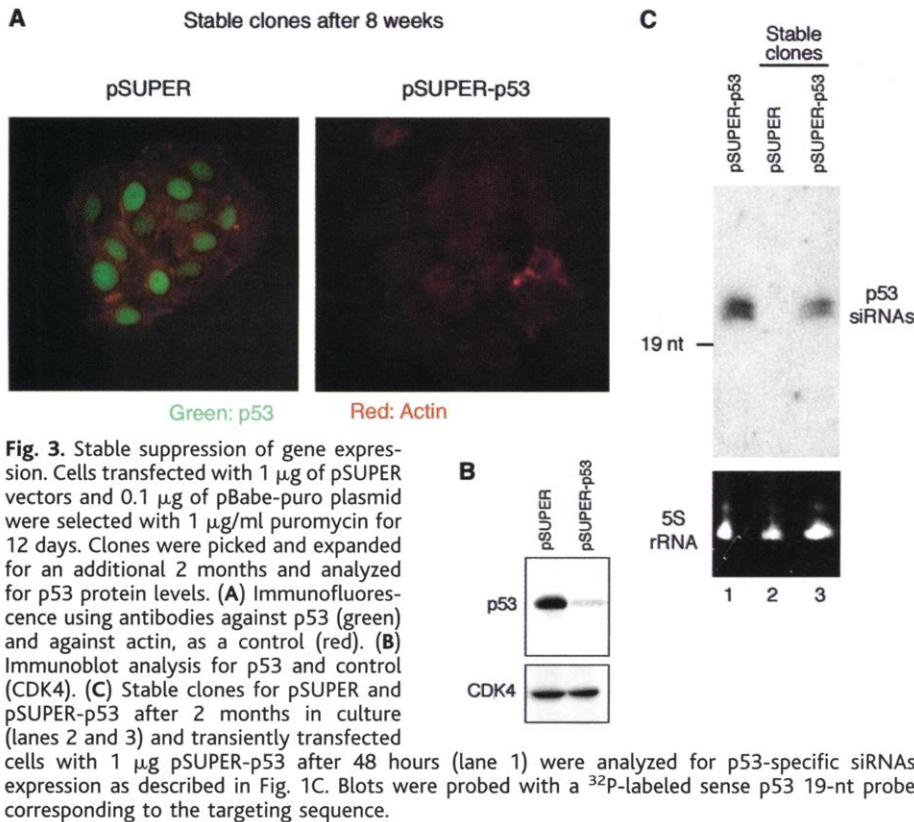


Fig. 3. Stable suppression of gene expression. Cells transfected with 1 μ g of pSUPER vectors and 0.1 μ g of pBabe-puro plasmid were selected with 1 μ g/ml puromycin for 12 days. Clones were picked and expanded for an additional 2 months and analyzed for p53 protein levels. **(A)** Immunofluorescence using antibodies against p53 (green) and against actin, as a control (red). **(B)** Immunoblot analysis for p53 and control (CDK4). **(C)** Stable clones for pSUPER and pSUPER-p53 after 2 months in culture (lanes 2 and 3) and transiently transfected cells with 1 μ g pSUPER-p53 after 48 hours (lane 1) were analyzed for p53-specific siRNAs expression as described in Fig. 1C. Blots were probed with a 32 P-labeled sense p53 19-nt probe corresponding to the targeting sequence.

expression by the pSUPER vector is sufficient to affect cellular physiology. We designed a construct to knockdown p53, a transcription factor that is stabilized following ionizing radiation (IR) and plays a crucial role in the maintenance of cell-cycle arrest in G_1 after DNA damage (7). Transfection of pSUPER-p53 reduced endogenous and overexpressed p53 protein [Fig. 1D, left, and Supplementary fig. 1B (4)] to very low levels and prevented entirely its induction after IR (Fig. 1D, left). Suppression of p53 was at the mRNA level, which was reduced by at least 90%, as judged by PhosphorImager quantification (Fig. 1D, middle). When vector-transfected cells were irradiated, they arrested within 24 hours in either G_1 or G_2 with very few cells remaining in S phase (Fig. 1D, right). In contrast, cells transfected with the pSUPER-p53 almost completely lost their p53-dependent arrest in G_1 but were able to establish a p53-independent G_2/M arrest. These results indicate that our vector can suppress endogenous p53 expression to the extent that it completely abrogates its function in the DNA damage response.

Finally, we asked whether the pSUPER vector can mediate stable suppression of gene expression. MCF-7 cells were co-transfected with a vector containing the puromycin-resistance marker and either pSUPER or pSUPER-p53. Cells were selected with puromycin, and resistant clones were cultured. When analyzed after 2 months, all pSUPER-transfected control clones stained brightly with p53-specific antibody, whereas more than 50% of pSUPER-p53 transfected clones showed significant reduction in p53 level (Fig. 3, A and B). In these stable clones p53-specific siRNA production was clearly detected (Fig. 3C, lanes 2 and 3) and was comparable to the level obtained after transient transfection of pSUPER-p53 (lane 1). These results indicate that the knockdown mediated by pSUPER is maintained over long periods and that its transcript products are not toxic to cells, as no selection against p53 knockdown was observed.

In summary, we provide a powerful new tool to stably suppress gene expression in mammalian cells, which will be useful in a variety of biological systems. Our finding that a single nucleotide mismatch in the 19-nt targeting sequence abrogates the ability to suppress gene expression also opens new avenues for gene therapy. Vectors that target disease-derived transcripts with point mutations, such as those from mutant *RAS* or *TP53* oncogenes, can now be specifically designed, without altering the expression of the remaining wild-type allele. In addition it should be possible to generate large collections of pSUPER siRNA vectors to carry out high-throughput genetic screens for loss-of-function phenotypes.

References and Notes

1. P. A. Sharp, *Genes Dev.* **13**, 139 (1999).
2. T. Hunter, T. Hunt, R. J. Jackson, H. D. Robertson, *J. Biol. Chem.* **250**, 409 (1975).

3. S. M. Elbashir *et al.*, *Nature* **411**, 494 (2001).
4. Supplementary material is available on *Science Online* at www.sciencemag.org/cgi/content/full/1068999/DC1.
5. M. Baer, T. W. Nilsen, C. Costigan, S. Altman, *Nucleic Acids Res.* **18**, 97 (1990).
6. T. R. Brummelkamp, R. Bernards, R. Agami, unpublished observations.
7. R. Agami, R. Bernards, *Cell* **102**, 55 (2000).
8. R. C. Lee, R. L. Feinbaum, V. Ambros, *Cell* **75**, 843 (1993).
9. We thank M. van Vugt for performing the PLK1 knock-down experiment and T. Tuschl for helpful discussion.

This work was supported by grants from the Dutch Cancer Society and the Center for Biomedical Genetics.

14 December 2001; accepted 26 February 2002
Published online 21 March 2002;
10.1126/science.1068999
Include this information when citing this paper.

A Thymic Precursor to the NK T Cell Lineage

Kamel Benlagha,¹ Tim Kyin,¹ Andrew Beavis,¹ Luc Teyton,² Albert Bendelac^{1*}

CD1d-restricted autoreactive natural killer (NK1.1⁺) T cells function as regulatory cells in various disease conditions. Using improved tetramer tracking methodology, we identified a NK1.1⁻ thymic precursor and followed its differentiation and emigration to tissues by direct cell transfer and in situ cell labeling studies. A major lineage expansion occurred within the thymus after positive selection and before NK receptor expression. Surprisingly, cytokine analysis of the developmental intermediates between NK⁻ and NK⁺ stages showed a T helper cell T_H2 to T_H1 conversion, suggesting that the regulatory functions of NK T cells may be developmentally controlled. These findings characterize novel thymic and postthymic developmental pathways that expand autoreactive cells and differentiate them into regulatory cells.

In addition to mainstream CD4 and CD8 $\alpha\beta$ T cells, the thymus produces specialized subsets of autoreactive regulatory cells, including CD1d-restricted CD4⁺ and CD4⁻8⁻ (DN) NK T cells and major histocompatibility complex (MHC) class II-restricted CD4⁺CD25⁺ cells. These cells exist at relatively high frequencies in peripheral tissues, where they regulate conventional T cell responses through the secretion of cytokines such as interleukin-4 (IL-4), IL-10, transforming growth factor- β , or interferon- γ (IFN- γ) [reviewed in (1, 2)]. Although little is known about the steps that govern the development of these cells, the study of T cell receptor (TCR) transgenic models has shown that the autoreactive nature of their TCRs is essential for their differentiation into regulatory cells (3, 4). However, direct study of the development of natural, nontransgenic regulatory cells has not been feasible because of their rarity and the lack of specific markers.

We focused on the developmental steps of the major population of regulatory NK T cells, which express the conserved V α 14-J α 18/V β 8 TCR (V α 24-J α 18/V β 11 in humans), and which regulate a broad range of disease conditions such as type I diabetes, cancer, and infections [reviewed in (5, 6)]. The development of these cells is particularly intriguing because they are a hybrid of the T and NK lineages, expressing both the $\alpha\beta$ TCR and the inhibitory MHC-

specific NK receptors (5, 6). Previous studies have shown that, unlike other autoreactive T cells, autoreactive NK T cells are not deleted in the thymus but are positively selected upon recognition of CD1d (presumably with an endogenous ligand) expressed by CD4⁺8⁺ cortical thymocytes (7, 8). The inherent autoreactivity of NK T cells seems to be controlled by the inhibitory NK receptors, because it is revealed in hybridomas lacking these NK receptors and in fresh cells exposed to dendritic cells (DCs) lacking the classical MHC class I ligands of these NK receptors (9, 10).

To study the developmental branchpoints of NK T cells relative to the T and NK lineages, the acquisition of T_H1 or T_H2 profiles, and the mechanisms underlying their high frequency in tissues, we identified these cells using tetramers of CD1d loaded with the synthetic lipid α -galactosylceramide (α GC). CD1d- α GC tetramers uniformly stain all NK T cells expressing the V α 14-J α 18/V β 8 TCR (11, 12). Because NK T cells are rare, nonspecific background staining is a problem; this can be partly overcome by simultaneous staining with empty CD1d tetramers (referred to as CD1d) conjugated with a different fluorochrome. After gating on CD1d- α GC⁺ CD1d⁻ thymocytes of 2-week-old B6 mice, the proportions of cells found were 0.08% in wild-type mice versus <0.01% in control J α 18^{-/-} mice (13) lacking NK T cells (Fig. 1A) (14). Nearly all of the cells were found among CD8⁻ thymocytes expressing low levels of the early cell surface marker HSA, whereas the few CD8⁺ cells were HSA^{high} and indistinguishable from background (as measured in J α 18^{-/-}). By focusing on these HSA^{low} cells in 2-week-old mice, we observed a predominance of NK1.1⁻

cells, as reported by others (15), in contrast to the predominantly NK1.1⁺ phenotype of their adult counterparts (Fig. 1B). Furthermore, nearly all of the NK1.1⁺ population could be separated into CD44^{low} and CD44^{high} subsets. Analysis of 3- and 6-week-old mice suggested a developmental sequence from CD44^{low}NK1.1⁻ to CD44^{high}NK1.1⁻ to CD44^{high}NK1.1⁺. Other NK lineage receptors (such as Ly49A, Ly49G/I, Ly49C, and CD94/NKG2) were also expressed late, along with or after NK1.1 (15, 16).

In situ labeling of thymocytes with fluorescein isothiocyanate (FITC) allowed the identification of recent emigrants in the spleen and liver (17). At 24 hours, most of these emigrants failed to express NK lineage markers and had the same CD44^{high}NK1.1⁻ phenotype as the thymic pre-NK1.1 stage (Fig. 2A). After 24 hours, a progressive expression of NK1.1 was observed (Fig. 2, A and B), suggesting that the thymic emigrants acquired the NK phenotype after entry into peripheral sites (18).

The frequency of V α 14 T cells among recent thymic emigrants was conspicuously high, at 4% in Fig. 2A and on average (16), and we estimate that as many as 1×10^5 V α 14 T cells could be exported to the spleen every day, a relatively large number compared with the size of the resident NK T population (5×10^5 to 10×10^5) (19).

To directly test the precursor-product relation between NK1.1⁻ and NK1.1⁺ cells, we sorted the NK1.1⁻ cells and transferred them intrathymically into J α 18^{-/-} hosts, which lack NK T cell precursors. We mixed into the inoculum 3% congenically marked, sorted NK1.1⁺ thymocytes (20) to rule out the possibility that a minor population of NK1.1⁺ contaminants could expand and account for the NK1.1⁺ cells found later. We found that most of the NK1.1⁻ cells expressed NK1.1 within a week, both in the thymus (Fig. 2C) and in the spleen and liver (16), whereas the congenically marked contaminants were not detectable. These results show that NK1.1⁻ cells represent precursors to those expressing NK1.1.

Because the thymic emigration experiments suggested a major expansion of V α 14 thymocytes before emigration, we examined the cell cycle status and turnover rate of NK T cell developmental intermediates (21). Indeed, we found that a large fraction of both CD44^{low}NK1.1⁻ and CD44^{high}NK1.1⁻ cells were actively dividing, as shown by the 16 to 18% bromodeoxyuridine-positive (BrdU⁺) cells at 12 hours and the 2.5 to 4.5% cells in S/M

¹Department of Molecular Biology, Princeton University, Princeton, NJ 08544, USA. ²Department of Immunology, Scripps Research Institute, La Jolla, CA 92037, USA.

*To whom correspondence should be addressed. E-mail: abendelac@molbio.princeton.edu